Machine and deep learning methods for detection and mapping of coastal wetlands of Crozon Peninsula (Brittany, France) used metric and sub-metric spatial resolution

Adrien Le Guillou, Simona Niculescu, Christiane Schmullius

Machine and deep learning methods for Detection and Mapping of coastal wetlands of Crozon Peninsula (Brittany, France) used metric and sub-metric spatial resolution

Le Guillou A. Author[a], Niculescu S. Author[a, b], and Schmullius C. Author[C]

[a]Univ Brest, CNRS, Nantes Université, Université de Rennes, LETG UMR 6554, F-29280 Plouzané, France
[b]Institut universitaire de France (IUF)
[c]Friedrich-Schiller-University Jena, Loebdergraben 32, 07743 Jena, Germany

ABSTRACT

Wetlands are one of the most important ecosystems in the world. Today, however, their fate is under serious threat, and their alarming decline highlights the urgent need to preserve these areas rich in biodiversity. The aim of this work is to spatially map and mapping the wetlands of the Crozon peninsula in Brittany France. The methodology is divided into two parts; the first part is to map the wetlands as a whole, while the second part is to mapping the wetlands using a adapted typology. Several databases were used to spatialise the wetlands: 12 Sentinel-2 images in L3A format, 23 Sentinel-1 VV and VH images and the RGE Alti (DTM at 1 metre resolution). The images were processed and stacked alone or in synergy. A random forest (RF) machine learning algorithm was then trained to predict wetlands in our study area using binary training data. The training data were obtained from a wetland inventory conducted in Brittany, distributed at the scale of a Sentinel-2 tile (30UUU). Post-processing was then carried out on the best result: binary morphological erosion and thresholding based on the DTM to remove outliers. We carried out two classifications, which we later merged. The classifications were carried out using a Pleiades time series (5 dates) to achieve a very fine scale classification. A classification of 13 land cover classes with 6 different wetland types (mudflats, salt marshes, coastal lagoons, wet meadows, wet forest, swamps/bogs) was performed using three methods: pixel-by-pixel random forest, object-based random forest and convolutional neural network (CNN). The best results obtained was for the pixel-based classification: kappa = 0.89, overall accuracy = 0.90, F1-score = 0.90.

Keywords: Wetland, Remote sensing, Machine learning, Deep learning, hydrology

1. INTRODUCTION

Wetlands cover about 6% of the Earth's surface.[1] These ecosystems are sources of numerous ecosystem services and benefit human society.[2] The number of wetlands has drastically decreased due to human pressure[3] .These areas have gradually been converted into farmland or urbanised areas. These changes affect biodiversity and contribute to the depletion of flora and fauna. Furthermore, wetlands help limit the impact of climate change.[4]

The first definition of a wetland in France came from the Water Act of 3 January 1992. This text defined wetlands as "land, whether used or not, that is usually permanently or temporarily flooded or inundated with fresh, salt, or brackish water; where vegetation exists, it is dominated by hygrophilous plants for part of the year" in Article L211-1 of the Environment Code. A number of criteria identify a wetland, e.g. vegetation specific to wetlands and/or soil that shows signs of waterlogging for at least part of the year. The criteria for delimiting a wetland can be found in the decree of 24 June 2008*.

Wetlands can be found on all types of land. These areas are located in the 283 communes of Finistère and account for 10% of the department's surface area (Conseil général du Finistère, 2011). Wetlands are found in

Further author information: (Send correspondence to Adrien Le Guillou.)
Adrien Le Guillou: E-mail: adrien.leguillou@univ-brest.fr
*Articles L. 214-7-4 and R. 211-108 of the Environment Code: https://www.legifrance.gouv.fr/loda/id/JORFTEXT000019151510

all reliefs, on plateaus, slopes, and valley bottoms, as well as in estuaries. These ecosystems can be peat bogs, meadows, forests, or mudflats.

Wetlands are a source of enormous benefits for human society. They provide a range of free services to society, commonly referred to as "ecosystem services".[5–8] Wetlands play a filtering role by improving water quality[9] ; they are a refuge for many plant and animal species[10] ; and they also play a "sponge" role by helping to prevent flooding and mitigate the effects of droughts.[11]

Unfortunately, these areas are seriously threatened by human activities. Wetlands are in decline. It is estimated that 64% of wetlands have been lost since 1900[12] and are disappearing three times faster than forests. Urban sprawl and agriculture are the main factors behind this decline.[13] Many practices have a destructive effect on wetland ecosystems, such as embankments, lack of maintenance, drainage, and the straightening of watercourses, all of which reduce the relationship between wetlands and watercourses.[14]

Several criteria can be used to identify wetlands. It is possible to determine whether an area is wet based on the characteristics of a habitat or a botanical criterion. Corine biotope habitats can be used for this.[15] It is also possible to identify a wetland based on the pedology of an ecosystem by determining whether one of the three main soil types characteristic of wetlands is present in the area: redox soil (temporary waterlogging), reductive soil (almost permanent waterlogging), or peaty soil (permanent waterlogging). Finally, the presence of wetland indicator species can also help identify wetlands. A national list of plant species that serve as wetland indicators was published by the decree of 24 June 2008 (Articles L. 214-7-1 and R. 211-108 of the Environment Code).

In the field of remote sensing, CNNs have become a powerful tool for analyzing satellite imagery data.[16–18] Satellite imagery provides a large amount of data, which requires efficient analysis techniques to extract relevant information .CNNs are suitable for this task as they can learn to recognise specific objects, structures and patterns in images.[19]

The advantages of CNNs in remote sensing are many. CNNs are capable of learning hierarchical features, meaning they can detect complex patterns at different levels of abstraction. In order to achieve this, convolutional layers use filters to identify local features from the input data, such as edges, textures, or even shapes in images.[20–22] In this way, small objects, such as buildings or vehicles, as well as larger structures, such as rivers or forests, can be identified[23][24] .

Remote sensing is a powerful tool for monitoring wetlands.[25,26] Thanks to its remote approach, it can acquire data over vast geographical areas, providing extensive spatial coverage and a global view of wetlands. With sensors mounted on satellites, aircraft or drones, images can be obtained at different resolutions,[27] allowing vegetation, hydrology and other environmental parameters to be characterised accurately and regularly.

One of the main advantages of remote sensing is its ability to provide data with high spatial and temporal resolution.[28] This makes it possible to observe seasonal and interannual changes in wetlands, detect variations in water extent, track changes in vegetation and monitor anthropogenic pressures.[29] This temporal resolution makes it possible to obtain up-to-date information on the condition of wetlands and understand their dynamics,[30] which is essential to supporting their conservation and sustainable management.[31]

Remote sensing offers the possibility of characterising wetland vegetation and habitats in detail[32].[33] By using different spectral bands and vegetation indices, it is possible to distinguish and map different vegetation types,[34] which allows a better understanding of their spatial distribution and interactions. In this way, changes in vegetation structure, land use and drainage networks can also be assessed, providing crucial information for water resource management and biodiversity conservation.[35]

This research aims to develop a reproducible methodology for the pre-location of wetlands using two methods. The first method is to locate wetlands using satellite images and elevation data. The second method is to be able to locate wetlands using an index calculated directly from elevation data (the topographic wetness index). Subsequently, a typology of wetlands using machine learning and deep learning methods will be produced. The objective of this research is also to better understand the dynamics of these areas and to study them on a sub-metric scale using Pleiades imagery (50 cm resolution).

Other research has been conducted on Crozon Peninsula. A study on the evolution of the peninsula's land use was carried out by Guanyao Xie and Niculescu[36] using machine and deep learning methods. Other paleontological

research on Crozon has also been undertaken, such as that of Vidal[37] or Perroud.[38] Numerous articles exist on the automatic mapping of wetland areas. Kulawardhana, proposed a methodology , including a two-part mapping.[39] Niculescu et al., 2016[40] showed that remote sensing contributes to the state of knowledge by understanding the interactions between optical signal, polarimetric radar signal, LiDAR measurements and wetlands in the Danube Delta. Niculescu et al., 2020. Niculescu et al., 2020[41] applied random forest from S2, Pleiades and S1 data and in situ observations for discrimination and mapping of reed against submerged aquatic vegetation (SAV), emergent macrophytes, some floating dicotyledonous plant communities and floating vegetation in deltaic lakes. In this study, a total of 67 classification models, in several combinations, with two sets of validation samples (with reed and without reed) were run. More recently in France, Rapinel et al., 2023 proposed similar research on a national scale, presenting a method for mapping wetlands using the topographic wetness index, among other techniques.[42] Huang et al., 2014 and Mao et al;, 2020 have conducted research on wetland mapping using Landsat images,[43,44] while other researchers like Bhatnagar have pursued similar themes using Sentinel-2 images.[45] Kaplan et al., 2017 and Mahdianpari et al., 2018, among others, have also contributed research on wetland mapping using a Sentinel-1/Sentinel-2 synergy.[46,47]

This study explores this subject in greater depth by adopting a methodology tailored to the study area, proposing a two-part cartographic approach, and exploring high spatial resolution imagery (Sentinel-2, ESA) as well as very high resolution imagery (Pléiades, Airbus DS). In addition, this study makes a scientific contribution to understanding land use in the wetlands of Finistère, a region that has been little studied on this subject until now. No sub-metre-scale study of wetland mapping using satellite images has been carried out in Brittany to date.

2. STUDY AREAS AND WETLANDS

2.1 Study area

The Crozon Peninsula is located in the far west of France, in the Brittany region. It is an integral part of the Parc naturel régionale d'Armorique. It is also a very maritime area, surrounded by the sea on all sides: the Brest Roadstead to the north, the Iroise Sea to the west and the Bay of Douarnenez to the south. Crozon is located at latitude 48.2477° N and longitude -4.4861° W. This area includes several towns and villages, such as the town of the same name, Crozon, as well as Roscanvel and Camaret-sur-Mer. The study area covers 104 km² of land. The topography of the peninsula is characterised by coastal diversity. There are numerous rocky cliffs, pebbled beaches, rocky foreshores, and fine sandy beaches. Land use is characterised by forests, moorland, meadows, farmland and urban areas. According to the Corine Land Cover database, there are 18 km² of urbanised areas, and according to BD Forêt®, there are 53 km² of woodland and shrubland, including 33 km² of moorland and 16 km² of deciduous land. Finally, according to RPG® 2021, there are 14 km² of agricultural land, mainly meadows. In Crozon, the urban fabric is not as predominant as in the rest of Brittany. Its natural areas are fairly well preserved thanks to the numerous military installations that have limited urban sprawl in Crozon.[48] The altitude varies, with a range of 329 m from the sea to Ménez Hom in the far east of the peninsula. The study area is not characterised by high altitudes, but the relief can still be marked by large degrees of slope. According to Météo France, the annual rainfall in 2021 was 1,043 mm (the national average in 2021 was 799 mm), with 1610 h of sunshine (the national average in 2021 was 1994 h). According to the Koppen classification, Crozon is classified as a "Cfb", or temperate oceanic climate.[49]

2.2 Wetland typology

There are many different types of wetlands, and each wetland can be divided into numerous ecological units. Habitat typologies such as CORINE biotopes, soil typologies such as GEPPA[50] which assesses soil hydromorphy), and environmental typologies such as RAMSAR[51] allow for more precise definitions of what constitutes a wetland. The wetland typology used in this study synthesises the different typologies mentioned above. The typology of these areas also focuses on the term "ecosystem", commonly defined as "a biological community interacting with organisms and their physical environment":

- Wet forests (or temperate rainforests) are characterised by abundant annual rainfall and moderate temperatures.[52] They are generally found in coastal regions, where oceanic air masses provide constant humidity,

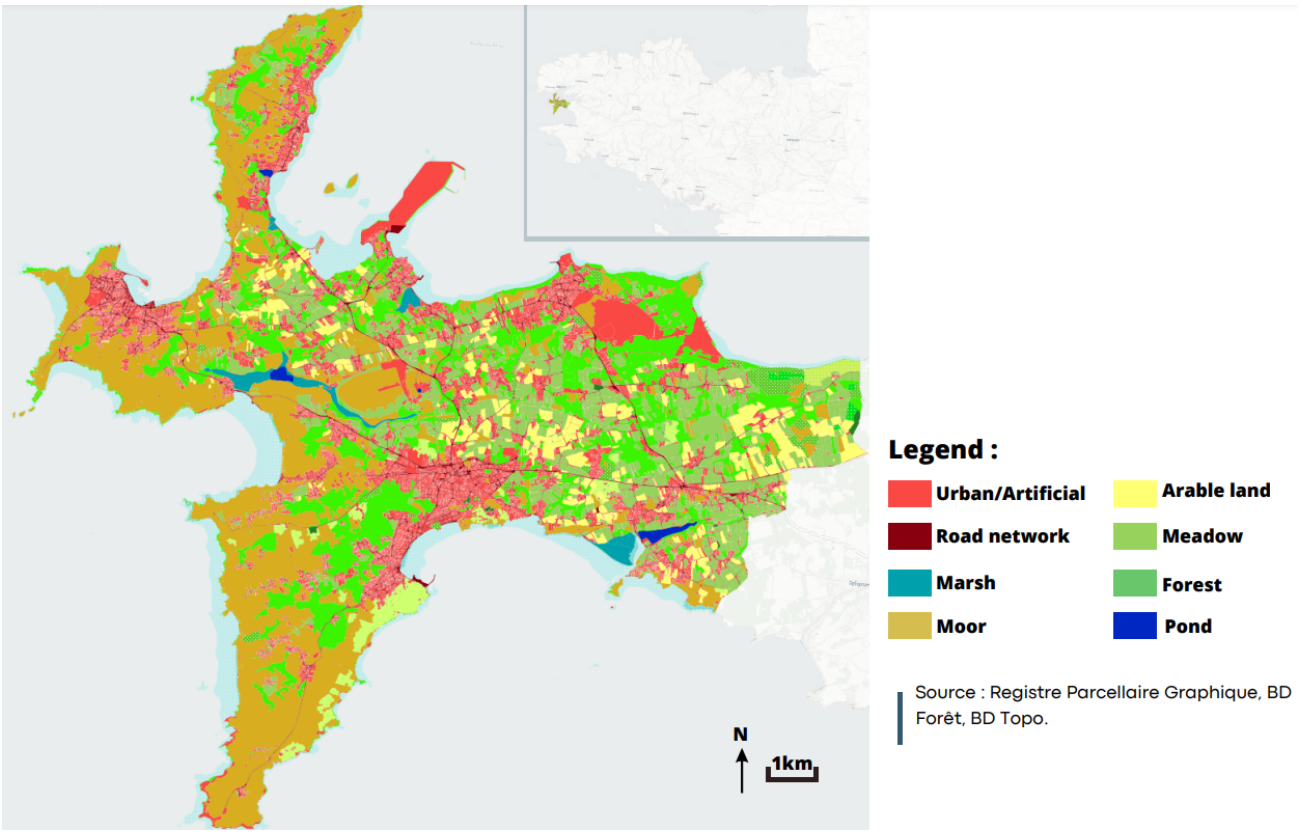

Figure 1: Location map of the Crozon peninsula

or in mountainous areas.[53] These forests consist of evergreen trees, such as conifers and broadleaf trees, which form a dense canopy.

- The wet meadow (or wet grassland) is an herbaceous ecosystem characterised by periodic or permanent soil saturation with water (redox or reductive soil). It is often found in topographical depressions where water accumulates after heavy rainfall or seasonal flooding.[54]
- Wet grasslands are home to a wide variety of herbaceous plants and grasses, such as rushes, that are specially adapted to waterlogged soils.
- A peat bog is an ecosystem characterised by an accumulation of partially decomposed organic matter, known as peat. It forms in regions where drainage conditions are very slow or nonexistent, allowing organic matter to be conserved. Peat bogs are rich in sphagnum moss and other plants adapted to acidic, nutrient-poor environments. They are essential habitats for specialised plant and animal species, and peat bogs are estimated to cover 3%–5% of the Earth's surface.[55]
- Salt meadows (or salt marshes) are coastal ecosystems located between land and high tide (intertidal zone[56]) .This environment is subject to regular fluctuations in water levels and is characterised by soils rich in mineral salts. The plants that grow here must be able to tolerate saline conditions. These areas are home to sea asters (*Tripolium pannonicum*) and obiones (*Obione portulaciodes*).
- Mudflats are intertidal coastal areas that are periodically covered and uncovered by tides.[57] These areas of sediment accumulation are rich in organic matter and fine sediment . Mudflats are home to a wide variety of plants, such as cord grass (*Spartina*), and animals adapted to shallow water and soft substrate.
- Finally, lakes or reservoirs are freshwater bodies formed naturally or through the construction of dams.

3. DATA IMPLEMENTED

The data used for this study are of several types: satellite images, an altimetry database and a wetland inventory. The satellite data used are as follows: Pleiades images (Airbus DS), Sentinel-2 images (Copernicus, ESA) and Sentinel-1 images (Copernicus, ESA).

3.1 Pleiades

The Pleiades constellation is a pair of Earth observation satellites. The constellation provides high-resolution satellite images captured by the Pleiades-1A and Pleiades-1B satellites. These satellites, initiated by Centre nationales d'études spatiales (CNES), provide a resolution of up to 0.5 m, making it possible to distinguish small details on the ground. The satellite images cover four spectral bands, ranging from the blue band in the visible spectrum to the near-infrared band. The high resolution enables detailed mapping, precise identification of objects and improved classification. This precision has many applications, including urban planning, environmental management and precision agriculture.

3.2 Sentinel

Sentinel-2 is a satellite mission for Earth observation within the European Union's Copernicus programme. It comprises a pair of satellites, Sentinel-2A and Sentinel-2B, which provide high-resolution, wide-field-of-view optical imaging data. The Sentinel-2 satellites provide a spatial resolution of up to 10 m in the visible spectral bands and up to 20 m in the infrared bands. They capture data in 13 different spectral bands, ranging from the visible to the near and mid-infrared. The mission offers a five-day global revisit to the equator and allows regular observations of areas of interest. Sentinel-2 data can also be accessed free of charge and without restrictions (available here: https://scihub.copernicus.eu/). Sentinel-1 is a satellite mission within the European Union's Copernicus programme that provides radar imagery data. It consists of two satellites, Sentinel-1A and Sentinel-1B, and uses synthetic aperture radar (SAR) technology. The Sentinel-1 satellites have active radar imaging capability, which means that they emit radar signals and record the echoes returned by the Earth's surface. This technology enables image acquisition independent of weather conditions and continuous observation day and night. Sentinel-1 offers two imaging modes: the interferometric (IW) mode, with a spatial resolution of 5 m, and the extra-wide (EW) mode, with a spatial resolution of 20 m. These different modes enable obtaining high-quality radar images and covering large areas relatively quickly.

3.3 Auxiliary data & altimetry data

In addition, external data was used to generate training and verification data based on a reference system. An inventory of wetlands in Brittany was used. These data are produced by the various SAGE (Schéma d'aménagement de gestion des eaux - water management development schemes) and are used to spatially classify the different wetlands. The Estimation de l'hydromorphie des sols (Estimation of soil hydromorphy) as reference data (database produced by UMR SAS INRA-Agrocampus Ouest) was also used[†]. Altimetric data in the form of a digital terrain model is also available with a 1-m resolution (RGE® Alti). Data processing for this paper was carried out using Qgis 3.22.12 (GDAL, SAGA and GRASS), OrfeoToolbox and SNAP.

4. METHODOLOGY

4.1 Image processing

In remote sensing, image processing is very important, especially before making a calculation[58] (classification, segmentation, etc...) . The images must be ready for use in different algorithms. Sentinel-1 and Sentinel-2 images (cf. Table1) were processed to map the wetlands.

First, the Sentinel-1 images were processed using SNAP software developed by ESA. The batch processing tool and the graph builder tool were used to automate the data processing in order to process the 22 Sentinel-1 images as quickly as possible. The chain used to process the Sentinel-1 data is as follows: Apply-Orbit-File,

[†]You can find the methodological guide for inventorying wetlands at the local level in the Finistère department at the following address:https://www.finistere.fr/var/finistere/storage/original/application/e17e923ab8d8c903be015a08e1c7c52f.pdf

Table 1: Satellite image data

Satellite	Number of image	Spectral bands	Spatial resolution
Sentinel-2	12 (L3A Format)	1,2(Blue),3(Green),4(Red), 5,6,7,8(NIR),8A,9,10,11,12	10 to 20m
Sentinel-1	22 (IW Format)	VV/VH	5x20m
Pléiades	5	1 (Blue), 2 (Green), 3 (Red), 4 (NIR)	0.50m
RGE Alti (DEM)	1		1m

ThermalNoiseRemoval, Calibration, SpeckleFilter and Terrain-Correction. Once the data has been processed, an extraction is performed with a mask corresponding to the study area, resulting in a ready-to-use Sentinel-1 image stack.

No specific processing was done for the Sentinel-2 images, as they were in L3A format. Since the L3A format is a monthly synthesis of Sentinel-2 L2A images, extensive image processing was performed in advance, resulting in a ready-to-use image after download. The L3A format provides a composite image made up of all the images captured on a Sentinel-2 tile over the month so that images with little or no cloud cover can be obtained. This is all thanks to the Sentinel-2 satellite's revisit capability.

However, in order to produce the best mapping of wetlands, many spectral indices have been calculated from Sentinel-2 images. Spectral indices are values calculated from reflectance measurements in different spectral bands of the Sentinel-2 images. These indices are used to characterise and analyse objects or phenomena in the images, such as vegetation, water resources and soils. They are calculated using specific mathematical formulas that exploit the differences in reflectance between the different spectral bands. In this case, we calculate mainly the spectral indices characterising vegetation and water resources to locate wetlands.

For the purpose of this article, seven spectral indices were calculated for the year 2021 based on the 30UUU tile:

- The normalised difference vegetation index (NDVI)[59] is the most widely used spectral index. It is used to assess the amount and condition of vegetation based on spectral data obtained from sensors on board satellites. The NDVI is calculated from reflectance measurements in the red (R) and near-infrared (NIR) spectral bands. The formula for calculating the NDVI is as follows:

$$NDVI = \frac{(NIR - R)}{(NIR + R)}.$$

- The green normalised difference vegetation index (GNDVI)[60] is used to estimate photosynthesis. This index determines water and nitrogen uptake in the plant canopy. The index is based on reflectance measurements in the green (G) and near-infrared (NIR) spectral bands:

$$GNDVI = \frac{(NIR - G)}{(NIR + G)}.$$

- The normalised difference water index (NDWI)[61] is one of the most widely used indices for delineating and evaluating water surfaces and resources and is particularly useful for detecting rivers and lakes. This index is based on short-wave infrared (SWIR) and near-infrared (NIR) bands:

$$NDWI = \frac{(NIR - SWIR)}{(NIR + SWIR)}.$$

- The bare soil index (BSI)[62] is used in remote sensing to identify and assess areas of bare or unvegetated soil. The combination of these spectral bands makes it possible to quantify the mineral composition of the

soil. This index is based on the red (R), short-wave infrared (SWIR), near-infrared (NIR) and blue (B) bands:

$$BSI = \frac{(R + SWIR) - (NIR + B)}{(R + SWIR) + (NIR + B)}.$$

- The advanced vegetation index (AVI)[62] is used to identify vegetation similar to the NDVI. The AVI aims to complete vegetation type discrimination by coupling the NDVI and the AVI. The index uses the red and near-infrared spectral bands:

$$AVI = [NIR \cdot (1 - R) \cdot (NIR - R)]^{\frac{1}{3}}.$$

- The automated water extraction index (AWEI)[63] is used to identify water resources in the same way as the NDWI. This index complements the information provided by the NDWI, particularly for river extraction. The AWEI calculation is based on reflectance measurements in the green (G), near-infrared (NIR) and short-wave near-infrared spectral bands:

$$AWEI = 4 \cdot (G - NIR) - (0.25 \cdot NIR + 2.75 \cdot SWIR).$$

- The transformed soil adjusted vegetation index (TSAVI)[63] is a vegetation index that attempts to minimise the influences of soil brightness by assuming that the soil line has an arbitrary slope and intercept, with X corresponding to the slope of the ground line, a corresponding to the intercept of the ground line and X corresponding to the adjustment defined to minimise ground noise. In this case, the value of $s = 0.33$, the value of $a = 0.5$ and the value of $X = 1.5$. The index uses the red (R) and near-infrared (NIR) bands:

$$TSAVI = \frac{s \cdot (NIR - s \cdot R - a)}{a \cdot NIR + R - a \cdot s + X \cdot (1 + s^2)}.$$

After all vegetation and water indices have been calculated, a stack is made between the Sentinel-1 and Sentinel-2 images in different combinations and the spectral indices (cf. Section 4.2).

4.2 Pre-location approach

In order to pre-locate and then map these areas, the method is divided into two parts. First, the wetlands are pre-located using altimetric and/or spectral data. This methodology allows the study area to be divided into two zones: "wetlands" and "non-wetlands". Two approaches were developed in order to achieve this methodology (cf. Figure 2).

The first method is based on the creation of a time series of Sentinel-1 and Sentinel-2 satellite images. The processed time series (calculation of spectral indices, Sentinel-1 processing on SNAP) is directly integrated into a random forest classification using training data from the inventory of wetlands (adapted to the scale of the Sentinel-2 30UUU tile) created for the Brittany region. The result is then post-processed with binary morphological erosion and thresholded with the RGE® Alti. Finally, after completing the entire processing chain, the best combination for pre-locating wetlands is selected. Six different combinations were tested (see Table 2).

The combination with the best metrics was kept (for validation, we used the wetland inventory described in Part 2.3). Another approach was developed to pre-locate wetlands in the study area. This approach primarily requires altimetric data in raster format. As mentioned previously, the RGE® Alti is used for processing (at a resolution of 1 m) in this case. From the RGE® Alti, we calculate the topographical wetness index[64] (cf. Figure 3) to estimate the areas where water will tend to merge and stagnate so that wetlands can be pre-located. When the results are available, thresholding is performed to extract all values corresponding to areas of stagnant water, resulting in a mask that pre-locates wetlands.

This index is used to create a raster model of water flow based on topographical data and can be used to represent potential water accumulation zones in a given area. The wetland inventory and the soil hydromorphy database were used to calculate the metrics and validate the results. It is important to note that the calculation of the topographical moisture index has some limitations, as this index does not take into account the nature of surface deposits, so it is mainly used to pre-locate "potential" wetlands.[65,66] To refine the result, we exclude the areas classified as wetlands that are located in impervious areas (urbanised areas or roads) by using a mask produced beforehand.

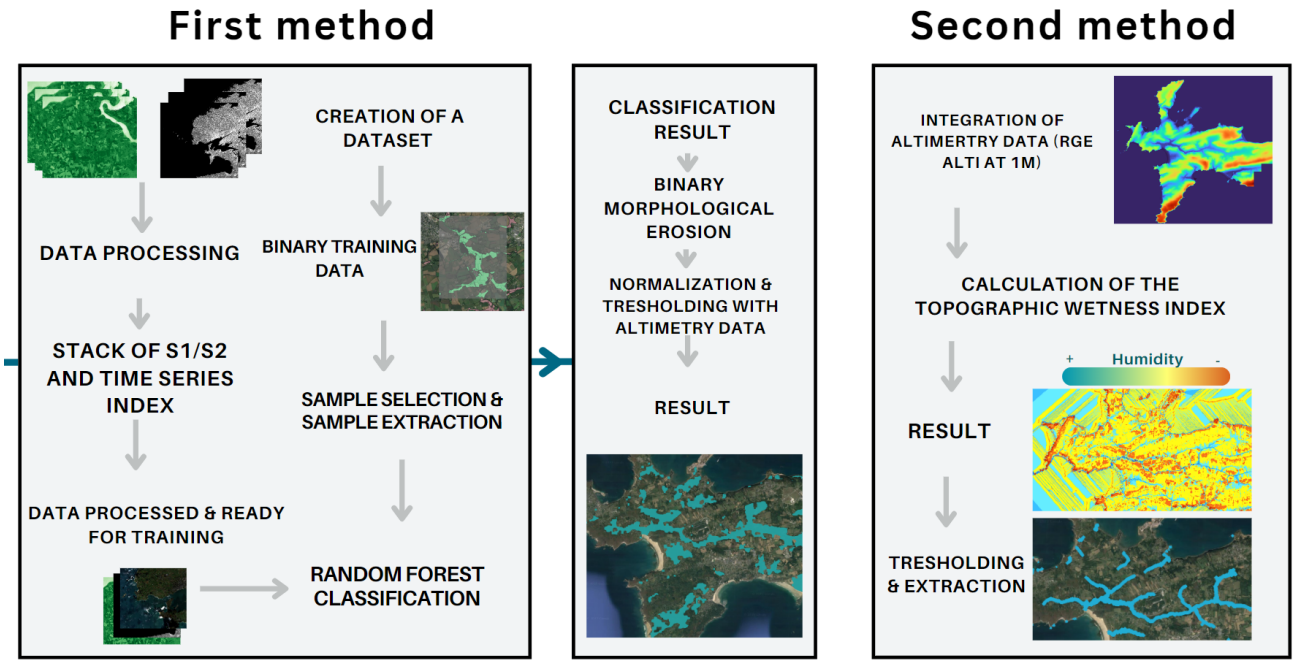

Figure 2: The two methodologies for pre-locating wetlands

Table 2: The different combinations for the first pre-location methodology

Method	Kappa	F1-Score	OA
Detection from : Stack Sentinel-2 and RGE Alti	**0.54**	**0.77**	**0.77**
Detection from Stack Sentinel-1	**0.60**	**0.79**	**0.80**
Detection using spectral indices : NDVI, GNDVI, NDWI , BSI, AVI, RGE Alti	**0.60**	**0.79**	**0.80**
Detection from : Synergy S1/S2 + RGE Alti	**0.57**	**0.78**	**0.78**
Detection using spectral indices : Previous indices + AWEI, TSAVI	**0.64**	**0.82**	**0.82**
Detection using : Standardised S2 stack	**0.54**	**0.75**	**0.76**

4.3 Mapping of wetlands

The second part of the methodology is based on a classification of land use in the two previously designated zones. There are now two zones, one corresponding to wetlands and the other to non-wetlands. It is important to note that only "continental" wetlands are considered in the wetland mask. Thus, we use the non-wetland mask to classify mudflats, as the topographical wetness index does not consider foreshores. The training data were generated using photo-interpretation of satellite images from 2021 (the date of classification) and external data such as BD Topo®, BD Ortho® and BD Forêt® (available free of charge on the Géoservice website[‡]). A homogeneous number of polygons (see Table 3) was implemented at the scale of the study area. The surface area of the training data was implemented as uniformly as possible, according to the type of land use in Crozon, as there are fewer peat bogs than in urban areas at the scale of the zone, so there is less surface area in training. This distribution also avoids overlearning and creating bias in the training data. Two land-use classifications are then produced.

[‡]https://geoservices.ign.fr/catalogue

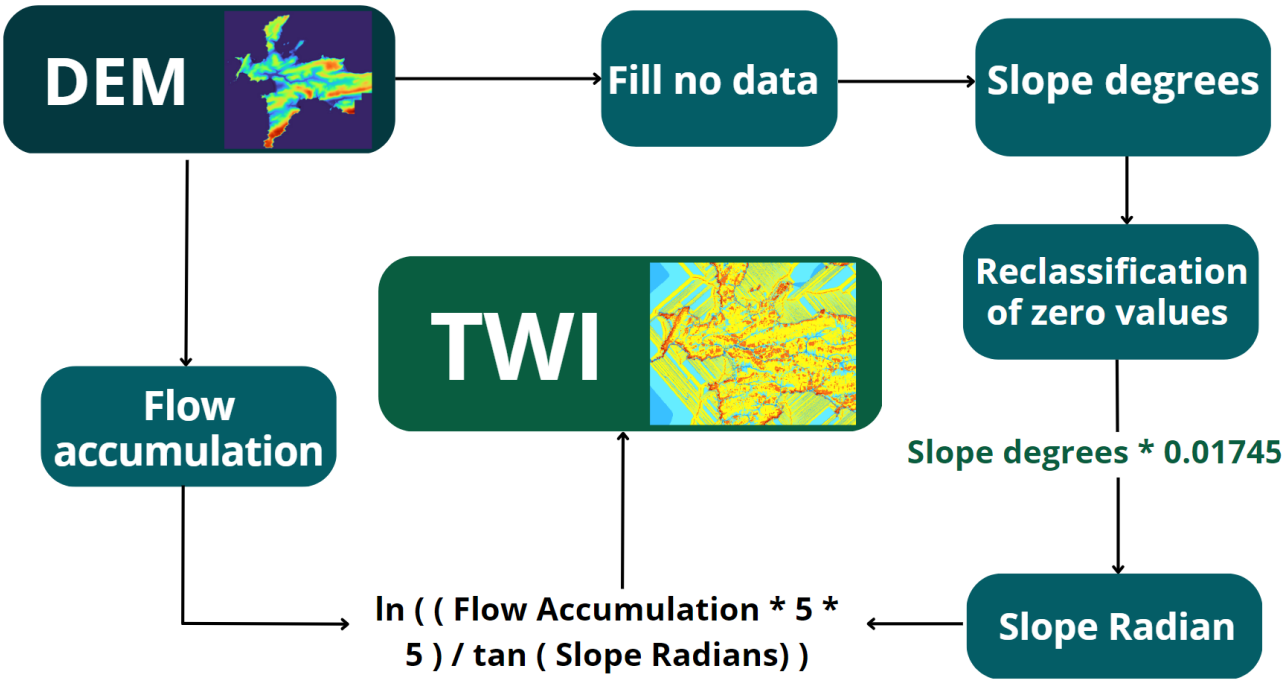

Figure 3: Methodology for Topographic Wetness Index calculation

Table 3: Training data surface area

Class	Area surface of training sample (m^2)
Wet meadow	26 899m^2
Mudflat	24 908m^2
Salt meadow	7 222m^2
Pond	28 484m^2
Marsh / Bog	6 074m^2
Wet Forest	29 003m^2
Rock / Cliff	17 692m^2
Urban / Artificial	140 912m^2
Arable Land	335 513m^2
Dry Heath	62 639m^2
Sand	113 223m^2
Deep water	920 764m^2
Forest and shrubland	57 767m^2

One was based on the "wetland" mask and the other on the "non-wetland" mask, and the two results were then merged to produce a complete map of the study area. Three types of classification were performed: two with machine learning algorithms and one with a deep learning algorithm. A pixel-by-pixel random forest classification and an object-based image analysis (OBIA) random forest classification were produced for the machine learning classifications. The convolutional neural network was chosen for the deep learning classification to create the land cover classification (cf. Figure 4). The neural network architecture is based on the documentation for the

Orfeotoolbox TensorFlow tool[§].[67]

5. MACHINE LEARNING

5.1 Random forest - Pixel by pixel and OBIA

The random forest is a reference model of machine learning for image processing. Proposed by Leo Breiman in 2001, this algorithm is based on a combination of decision trees. It is the model most often used for classification, given its performance and speed of execution compared to other machine learning algorithms.[68] The random forest also has the advantage of being easy to use.[69] Random forest functions as a set of decision trees used to predict a quantity or probability. The decision tree alone is a tool in the form of a tree (which can resemble a flowchart), where each node is a test for an attribute, and the branch is an outcome. A tree is divided into a "source" set and then into subsets. This process is repeated for each subset in recursive form.

We need three "hyper-parameters"[70] (fixed parameters) to be defined before training. These are the size of the trees (maximum number of nodes), the number of trees and finally, the number of features to be sampled (number of random variables selected from the explanatory variables in each mixture). The first step involves implementing the "bagging" principle,[71] i.e. creating numerous random subsamples on a subset of the data. The second step is to develop individual decision trees for each sample. The different trees are trained by a random portion to make a prediction. It is important to note that each decision tree works individually and independently. Finally, the third step corresponds to the results of the predictions and is the result of the majority vote, which is the final prediction. Our random forest has the following parameters: maximum number of decision trees: 200, minimum number of samples per class: 20, and maximum depth of decision trees: 10. A time series of five Pleiades images was used for the random forest approach. As part of this research, random forest was implemented with two different classification methods: the pixel approach and the object approach.

Pixel approach

The pixel approach uses a learning algorithm to automatically extract the characteristics of pixels and associate them with classes (in this case, land-use classes). The principle of this approach is to use the spectral information of the pixels in one or more satellite images that have already been labelled and are therefore known. Once a sufficient number of pixels have been labelled, they are implemented in a machine-learning model to produce a trained model. Once the model has been trained, it can be applied to an entire satellite image (or time series), and a class prediction is made for each pixel in the image.

Object approach

In the object approach,[72,73] neighbouring pixels with similar characteristics are grouped together (e.g. a house consisting of pixels with a similar spectral response is grouped to form an "object"). Colour, texture and spatial context can all influence the creation of the "object". There are many different segmentation algorithms, e.g. mean shift[74] or nearest neighbour.[75] Once the objects have been segmented, specific descriptors are extracted for each object, considering characteristics such as size, shape, texture, colour, etc. These descriptors are used as inputs for the object and then as inputs for machine learning algorithms, in our case, random forest. The meanshift method was used for our object approach. We chose the following parameters to produce our segmentation: spatial radius: 10, range radius: 30, maximum number of iterations: 50, minimum "region" size: 200, minimum object size: 5, and polygon simplification: 0.5.

5.2 Deep learning principles

Deep learning is a discipline of artificial intelligence that uses deep artificial neural networks to solve complex problems.[76–79] These networks are capable of learning from raw data and extracting abstract representations. Deep learning is based on iterative supervised or unsupervised learning processes where networks are trained on labelled data or to discover structures in unlabelled data.[80]

Deep learning has wide applications in areas such as computer vision[81] ,natural language processing,[82] speech recognition,[83] machine translation and robotics.[84] For example, deep neural networks are used in computer vision

[§]To use OTBTF: https://otbtf.readthedocs.io/en/latest/

for object detection,[85] facial recognition and image segmentation.[86] In natural language processing, deep learning is used for tasks such as text classification,[87] text generation and machine translation.[88]

However, deep learning also presents challenges and limitations. One major challenge is the need for large amounts of labelled data to efficiently train deep neural networks. The interpretability of learned models is also challenging, as deep neural networks are often considered "black boxes" due to their complexity.[89] In addition, deep learning can face the problems of overlearning[90] and limited generalisation in situations where the training data differs from the real data

5.3 Architecure of the CNN

The CNN model proposed in this article consists of several layers for processing the input images (see Figure 4). The training data were generated from a Pleiades image, for which 5000 16-by-16 patches were extracted for each land cover class, and 5000 additional patches were used for validation. The architecture of CNN is as follows: The image patches have a resolution of 16 x 16 and are subjected to a series of three convolution layers. The first convolution layer with 16 filters of size 5 x 5 is followed by a ReLU activation function and a pooling layer of size 2 x 2. A second convolution layer with 16 filters of size 3 x 3 is then applied, followed by another pooling layer. Finally, a third convolution layer with 32 filters of size 2 x 2 is used. A test with 64 x 64 patches is also performed. The extracted features are then reshaped into a vector and fed into a fully connected layer. This latter layer consists of six or seven neutrons (depending on the "wetland" or "non-wetland" mask, which is not characterised by the same classes) corresponding to the predicted classes. The predicted class was determined by selecting the index of the neuron with the highest output value (e.g. a probability). The model is trained by minimising the loss using the cross-entropy cost function. The optimisation is performed with the Adam optimiser.

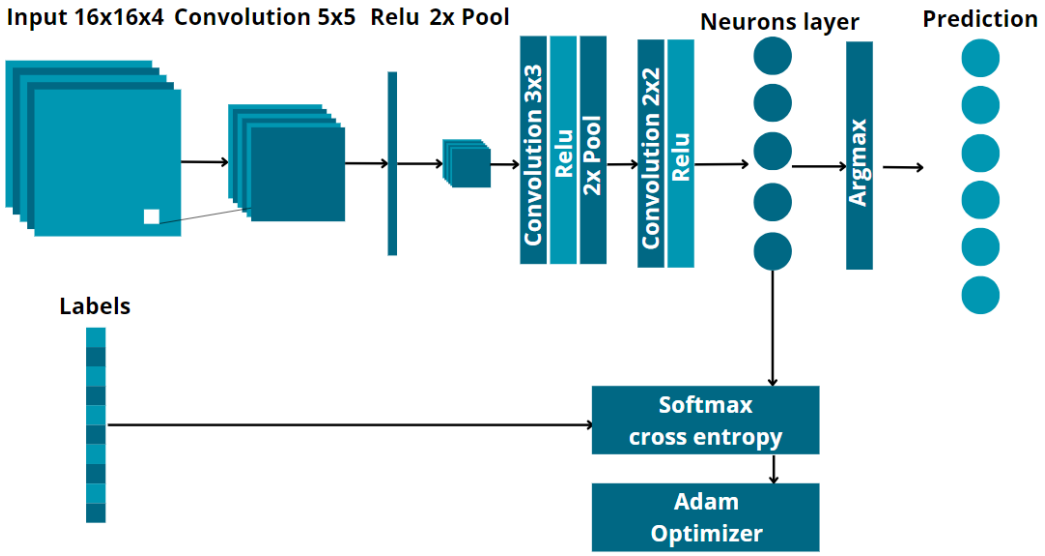

Figure 4: Architecture of the CNN

6. EVALUTATION OF CLASSIFICATIONS

6.1 Pre-location of wetlands

The first step in the wetland classification methodology was to locate all the wetlands, for which two methods were developed. The first method was based on spectral indices (see Section 4.1), and the second on the topographical wetness index (TWI). The method using the TWI works best. The wetland inventory (made by

local actors)[¶] and soil hydromorphy map (made by Agrocampus Ouest, INRA SAS)[‖] were used as validation datasets to evaluate the best method. The metrics show higher scores for the TWI, with a difference of +0.04 for the F1-score, +0.26 for the kappa, and +.10 (cf. Table 5) for the overall accuracy. Visually, the pre-location also appears better, with more relevant flow lines. In addition, the TWI method has the advantage of being less costly in terms of computation time, as it does not require classification with an extensive training dataset but only calculations based on altimetric data.

Table 4: Score of the two methods for pre-loating wetlands

Methods	**Spectral index**	**TWI**
F1-Score	0.82	0.86
Kappa	0.64	0.90
OA	0.82	0.92

In order to validate the different results, a validation dataset independent of the training dataset was created. For this purpose, 30% of the polygons initially intended for training were separated to form the validation dataset. Next, 1,000 points per land-use class were extracted for validation. The same validation dataset was used for the different approaches to have comparable reference data. Three classifications were tested with three different approaches. The pixel-by-pixel random forest approach achieved the best results of the different classifications, followed by the convolutional neural network and, finally, the OBIA random forest approach (cf. metric table). The only exception is the F-1 score, for which the CNN achieved the best score with a difference of 0.01 compared to the pixel approach.

Table 5: Score for the three wetlands mapping approaches

	OBIA RF	**Pixel by Pixel RF**	**CNN**
OA	**0.85**	**0.89**	**0.87**
Kappa	**0.84**	**0.90**	**0.86**
F1-Score	**0.76**	**0.82**	**0.83**

By looking more closely at the metrics using the confusion matrix (a matrix produced with the "ComputeConfusionMatrix" tool in OrfeoToolbox), it is possible to examine the confusion between classes. Wetlands are well classified overall, thanks in part to the "wetland" mask, which prevents confusion between the "wet forest" and "forest" classes or between the "wet meadow" and "agricultural land" classes.

The convolutional neural network showed better metrics for the "mudflat" class, with less confusion with the "rock/cliff" class than the random forest classification. Conversely, the "forest" class performed worse for the neural network than the random forest, with high confusion with the "dry heat" class. This is probably due to the similar reflection of shrubby areas in moorlands and small trees in forests.

The random forest classification with the pixel approach shows very good metrics overall, as does the OBIA approach. However, there is some confusion between the "rock/cliff" and "artificial land" classes. This confusion is quite understandable, given the similar reflectance between a rocky coastline and roads. This confusion can also be observed with CNN, but to a lesser extent. Confusion is also visible between the "sand" and the "artificial land" classes, both at OBIA and in the pixel approaches.

In short, the random forest approach shows better discrimination for land-use classes linked to wetlands, while the neural network performs better for areas outside wetlands. This is primarily due to better discrimination between the "sand", "artificial land" and "rock/cliff" classes.

Visually (cf. Figure 5), the random forest pixel approach shows a more accurate mapping than the OBIA or CNN classification. CNN tends to have a "salt and pepper" effect. This effect may be due to the size of the patches entered, which does not allow for sufficiently precise segmentation at the scale of the resolution of the

[¶]https://bretagne-environnement.fr/donnees-zones-humides-bretagne

[‖]Hydromorphy soil : https://sols-de-bretagne.fr/inventaire-et-cartographie-sols/applications-thematiques/192-hydromorphie-des-sols.html

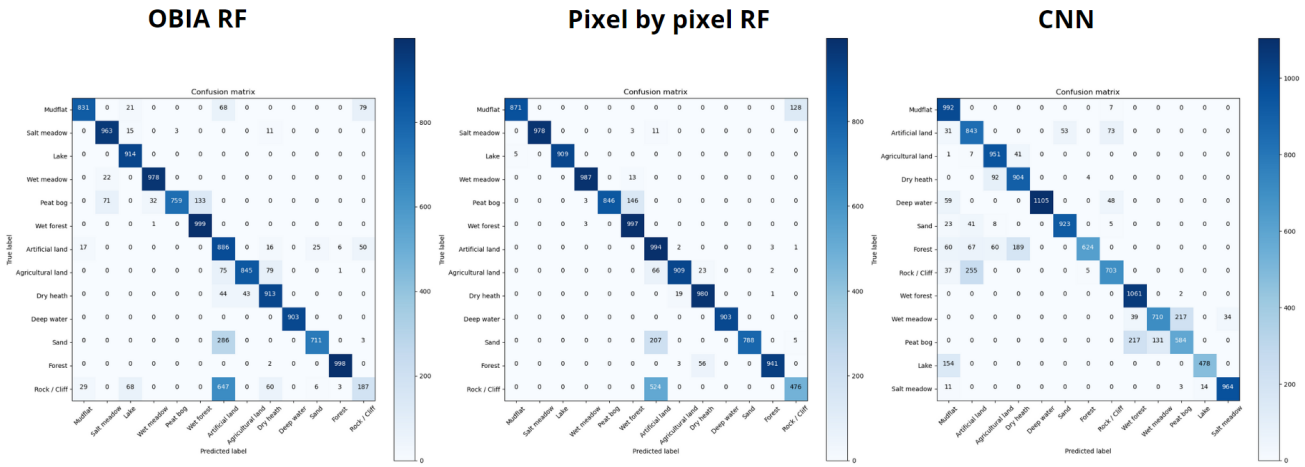

Figure 5: Confusion matrix for the three wetlands classifications

Pleiades images. Finally, the OBIA classification provides a visually relevant map, but one that exhibits tiling effects (i.e. a spatial discontinuity between two land cover classes). This effect is particularly noticeable between the "lake" class and the "deep water" class, where it is possible to see pixels classified as "lake" in the form of a square in an area that should normally be "deep water". The OBIA classification also tends to overrepresent the "artificial land" class (predominance of red on the map). Many pixels are classified as "artificial land" when, in fact, they are "sand" or "rock/cliff" that can be seen directly on the coastline or beaches.

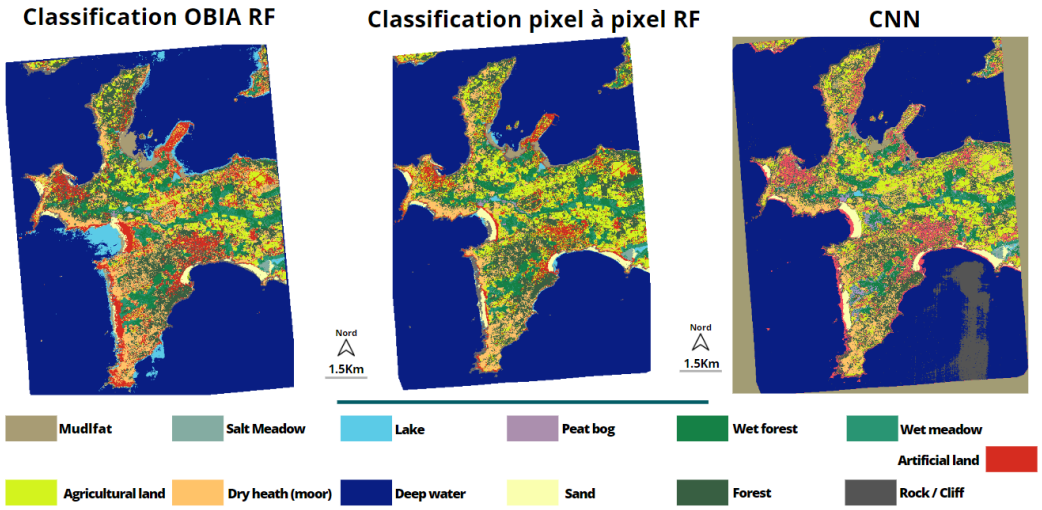

Figure 6: The three land use classifications

7. DISCUSSION & PERSPECTIVES

7.1 Discussion

The results therefore show that the methodology described in this article is capable of mapping wetlands. With scores ranging from 0.76 (OBIA, F1-score) to 0.90 (pixel, kappa), the metrics show fairly satisfactory results, with an OA of 89% for the pixel random forest approach. The two-stage approach involves pre-locating wetlands using spectral indices or the topographical moisture index (TWI). By mapping the different wetland typologies using the pre-location mask, it is then possible to reduce the confusion between the different land-use classes. The best classification is the pixel-by-pixel random forest classification, although this approach is similar to

that of the neural network (in terms of metrics). These two classifications have a difference of 0.04 for the kappa, 0.02 for the overall accuracy (in favour of the RF) and 0.01 for the F1-score (in favour of the CNN). Nevertheless, the pixel-by-pixel random forest classification visually appears better than the OBIA and CNN approaches. Numerous research studies have shown that deep learning is able to obtain better scores as a general rule compared with more "traditional" machine learning algorithms.[91–94] However, in the case of this article, the pixel approach shows slightly higher scores. This may be due to the architecture of the neural network, which could be improved by integrating more convolution and hidden layers. It is also possible to integrate patches with larger entries (64x64, 128x128 for example) or to integrate more images in the Pleiades time series. It is also important to note that the computation time for deep learning is significantly higher than for machine learning algorithms and requires more hardware resources (graphics card). This energy cost is not to be overlooked, and may call into question the use of this tool depending on the real need for it.[95]

Improvements can still be made to the methodology. The use of new spectral indices or new algorithms could probably refine the results for pre-locating wetlands. For the classification and typology of wetlands, neural networks could offer significant potential for improvement. To this end, a comparative study of the best deep learning algorithm architectures can be carried out with a view to implementing them in a land use classification.

This study shows good results for the wetland classes studied. For the random forest pixel method, the wetland classes achieve an average Overall Accuracy score of 93% (see comparative table of scores). A similar study by Ouyang et al. was published, investigating the comparison between a pixel-based approach and an Object-Based Image Analysis (OBIA) approach for saltmarsh vegetation mapping. This study shows scores (in Overall Accuracy) ranging from 78% to 82% for their approach, using QuickBird images for a similar class study as ours (Mudflat with Spartina and Saltmarsh with Phragmites).[96] Another more recent study by Mahdianpari et al., on urban wetland mapping, was published. This study shows results similar to ours, achieving an OA of 91% for similar wetland land cover classes. The study utilizes WorldView-4, GeoEye-1, and LiDAR data to characterize wetlands into five classes: Bog, Fen, Swamp, Marsh, and Open Water.[97]

7.2 Perspectives

There are possible avenues for improvement in this work. Initially, the convolutional neural network is the best candidate for improvement. Many improvements can be made to the neural network's architecture, such as implementing more convolution layers or changing the gradient descent. In short, it is possible to conduct research that focuses entirely on neural networks and try out the architecture that would be most suitable[98] so that architectures such as the U-Net,[99] the VGG-Net[100] and the LoopNet can be evaluated. Besides the deep learning aspect, it is also possible to delve deeper into the machine learning aspect by trying other algorithms, such as support vector machines.[101] It is also possible to implement a larger input dataset. The training dataset was 5,000 t per land-use class; it is possible to use 10,000 t per land-use class to investigate whether an improvement is visible with a larger input dataset.

In the case of the pre-location of wetlands, it is also possible to try new approaches or new indices. If the goal is still to use spectral information for pre-location, indices like the modified soil-adjusted vegetation index (MSAVI)[102] or the enhanced vegetation index (EVI)[103] can be included in the methodology to determine how useful their contributions are. The use of other wetness indices can also be tested, as not only the topographic wetness index can be used to spatially delineate areas that are likely to be wet. The vertical distance to channel network (VDCN)[104] is also an algorithm that can be used to model flow lines to identify areas that are likely to be wet or under water.

8. CONCLUSION

The proposed methodology made it possible to map wetlands in various ways and with different approaches, with an accuracy between 76% and 90%. The aim of this research was also to develop a reproducible methodology for as many different landscapes as possible. In this way, the methodology can be reused in different areas using altimetric data and satellite images, regardless of the spatial and spectral resolution of the sensor. The advantage of pre-locating wetlands is that the study can be divided into two parts, reducing the confounding of land-use classes with similar spectral responses. By dividing the study area into two groups (wetland mask and non-wetland mask), confusion between forest and wetland forest classes could be avoided, allowing for better

classification. This article highlights a number of significant strengths resulting from in-depth analyses. The methodologies used have produced convincing results in the analysis and fine mapping of wetlands, making a contribution to the field of study. With precise data and good results, this article provides additional elements in the spatial understanding of wetlands, opening up promising new prospects for this theme. Land-use classes for wetlands based on several typologies (RAMSAR, GEPPA) make it possible to discriminate between wetlands with precision. This typology also provides a methodology that can be reproduced in several stages to produce its own wetland maps. Mapping in two stages (pre-location and mapping) has the advantage of being able to improve discrimination between wetlands and non-wetlands. It also provides geospatial information for the area under study (Crozon, France).

ACKNOWLEDGMENTS

This research was funded by the the project CNES (Centre national d'études Spatiales) / TOSCA 7618.

REFERENCES

[1] Erwin, K. L., "Wetlands and global climate change: the role of wetland restoration in a changing world," *Wetlands Ecology and management* **17**(1), 71–84 (2009).

[2] Clarkson, B. R., Ausseil, A.-G. E., Gerbeaux, P., et al., "Wetland ecosystem services," *Ecosystem services in New Zealand: conditions and trends. Manaaki Whenua Press, Lincoln* **1**, 192–202 (2013).

[3] Boesch, D. F., Josselyn, M. N., Mehta, A. J., Morris, J. T., Nuttle, W. K., Simenstad, C. A., and Swift, D. J., "Scientific assessment of coastal wetland loss, restoration and management in louisiana," *Journal of Coastal Research* , i–103 (1994).

[4] Salimi, S., Almuktar, S. A., and Scholz, M., "Impact of climate change on wetland ecosystems: A critical review of experimental wetlands," *Journal of Environmental Management* **286**, 112160 (2021).

[5] Barbier, E. B., "Valuing ecosystem services for coastal wetland protection and restoration: Progress and challenges," *Resources* **2**(3), 213–230 (2013).

[6] Koch, E. W., Barbier, E. B., Silliman, B. R., Reed, D. J., Perillo, G. M., Hacker, S. D., Granek, E. F., Primavera, J. H., Muthiga, N., Polasky, S., et al., "Non-linearity in ecosystem services: temporal and spatial variability in coastal protection," *Frontiers in Ecology and the Environment* **7**(1), 29–37 (2009).

[7] Twilley, R. R., "Coastal wetlands & global climate change," *Gulf coast sustainability in a changing climate. Regional Impacts of Climate Change: Four Case Studies in the United States. 24pp* (2007).

[8] Farber, S., "The value of coastal wetlands for protection of property against hurricane wind damage," *Journal of Environmental Economics and Management* **14**(2), 143–151 (1987).

[9] Wallace, J. and Waltham, N. J., "On the potential for improving water quality entering the great barrier reef lagoon using constructed wetlands," *Marine Pollution Bulletin* **170**, 112627 (2021).

[10] Boesch, D. F. and Turner, R. E., "Dependence of fishery species on salt marshes: the role of food and refuge," *Estuaries* **7**, 460–468 (1984).

[11] Maltby, E. and Acreman, M. C., "Ecosystem services of wetlands: pathfinder for a new paradigm," *Hydrological Sciences Journal* **56**(8), 1341–1359 (2011).

[12] Davidson, N. C., Fluet-Chouinard, E., and Finlayson, C. M., "Global extent and distribution of wetlands: trends and issues," *Marine and Freshwater Research* **69**(4), 620–627 (2018).

[13] Ballut-Dajud, G. A., Sandoval Herazo, L. C., Fernández-Lambert, G., Marín-Muñiz, J. L., López Méndez, M. C., and Betanzo-Torres, E. A., "Factors affecting wetland loss: A review," *Land* **11**(3), 434 (2022).

[14] Costanza, R., Farber, S. C., and Maxwell, J., "Valuation and management of wetland ecosystems," *Ecological economics* **1**(4), 335–361 (1989).

[15] Bissardon, M., Guibal, L., and Rameau, J., "Corine biotopes, types d'habitats français," *Nancy, ENGREF-ATEN* **175** (1997).

[16] Kattenborn, T., Leitloff, J., Schiefer, F., and Hinz, S., "Review on convolutional neural networks (cnn) in vegetation remote sensing," *ISPRS journal of photogrammetry and remote sensing* **173**, 24–49 (2021).

[17] Ren, Y., Zhu, C., and Xiao, S., "Small object detection in optical remote sensing images via modified faster r-cnn," *Applied Sciences* **8**(5), 813 (2018).

[18] Bhosle, K. and Musande, V., "Evaluation of deep learning cnn model for land use land cover classification and crop identification using hyperspectral remote sensing images," *Journal of the Indian Society of Remote Sensing* **47**(11), 1949–1958 (2019).

[19] Deng, Z., Sun, H., Zhou, S., Zhao, J., Lei, L., and Zou, H., "Multi-scale object detection in remote sensing imagery with convolutional neural networks," *ISPRS journal of photogrammetry and remote sensing* **145**, 3–22 (2018).

[20] Albawi, S., Mohammed, T. A., and Al-Zawi, S., "Understanding of a convolutional neural network," in [*2017 international conference on engineering and technology (ICET)*], 1–6, Ieee (2017).

[21] Koushik, J., "Understanding convolutional neural networks," *arXiv preprint arXiv:1605.09081* (2016).

[22] Yoo, H.-J., "Deep convolution neural networks in computer vision: a review," *IEIE Transactions on Smart Processing & Computing* **4**(1), 35–43 (2015).

[23] Zhang, S., Wu, R., Xu, K., Wang, J., and Sun, W., "R-cnn-based ship detection from high resolution remote sensing imagery," *Remote Sensing* **11**(6), 631 (2019).

[24] Hsu, S.-C., Huang, C.-L., and Chuang, C.-H., "Vehicle detection using simplified fast r-cnn," in [*2018 International Workshop on Advanced Image Technology (IWAIT)*], 1–3, IEEE (2018).

[25] Guo, M., Li, J., Sheng, C., Xu, J., and Wu, L., "A review of wetland remote sensing," *Sensors* **17**(4), 777 (2017).

[26] Demarquet, Q., Rapinel, S., Dufour, S., and Hubert-Moy, L., "Long-term wetland monitoring using the landsat archive: A review," *Remote Sensing* **15**(3), 820 (2023).

[27] White, J. C., Coops, N. C., Wulder, M. A., Vastaranta, M., Hilker, T., and Tompalski, P., "Remote sensing technologies for enhancing forest inventories: A review," *Canadian Journal of Remote Sensing* **42**(5), 619–641 (2016).

[28] Li, X., Ling, F., Foody, G. M., Ge, Y., Zhang, Y., and Du, Y., "Generating a series of fine spatial and temporal resolution land cover maps by fusing coarse spatial resolution remotely sensed images and fine spatial resolution land cover maps," *Remote Sensing of Environment* **196**, 293–311 (2017).

[29] Wuver, A., "The impact of human activities on biodiversity conservation in a coastal wetland in ghana," *West African Journal of Applied Ecology* **9**(1) (2006).

[30] Qin, P. and Zhang, Z., "Evolution of wetland landscape disturbance in jiaozhou gulf between 1973 and 2018 based on remote sensing," *European Journal of Remote Sensing* **54**(sup2), 145–154 (2021).

[31] Copeland, H. E., Tessman, S. A., Girvetz, E. H., Roberts, L., Enquist, C., Orabona, A., Patla, S., and Kiesecker, J., "A geospatial assessment on the distribution, condition, and vulnerability of wyoming's wetlands," *Ecological Indicators* **10**(4), 869–879 (2010).

[32] Ozesmi, S. L. and Bauer, M. E., "Satellite remote sensing of wetlands," *Wetlands ecology and management* **10**, 381–402 (2002).

[33] De Roeck, E. R., Verhoest, N. E., Miya, M. H., Lievens, H., Batelaan, O., Thomas, A., and Brendonck, L., "Remote sensing and wetland ecology: a south african case study," *Sensors* **8**(5), 3542–3556 (2008).

[34] Huete, A. R., "Vegetation indices, remote sensing and forest monitoring," *Geography Compass* **6**(9), 513–532 (2012).

[35] Bastiaanssen, W. G. et al., [*Remote sensing in water resources management: the state of the art.*], International Water Management Institute (1998).

[36] Xie, G. and Niculescu, S., "Mapping and monitoring of land cover/land use (lclu) changes in the crozon peninsula (brittany, france) from 2007 to 2018 by machine learning algorithms (support vector machine, random forest, and convolutional neural network) and by post-classification comparison (pcc)," *Remote Sensing* **13**(19), 3899 (2021).

[37] Vidal, M., Dabard, M.-P., Gourvennec, R., Le Hérissé, A., Loi, A., Paris, F., Plusquellec, Y., Racheboeuf, P., et al., "Le paléozoïque de la presqu'île de crozon, massif armoricain (france)," *Géologie de la France* **1**, 3–45 (2011).

[38] Perroud, H., Bonhommet, N., and Van der Voo, R., "Palaeomagnetism of the ordovician dolerites of the crozon peninsula (france)," *Geophysical Journal International* **72**(2), 307–319 (1983).

[39] Kulawardhana, R., Thenkabail, P. S., Vithanage, J., Biradar, C., Islam, A., Gunasinghe, S., and Alankara, R., "Evaluation of the wetland mapping methods using landsat etm+ and srtm data.," *Journal of Spatial Hydrology* **7**(2) (2007).

[40] Niculescu, S., Lardeux, C., Grigoras, I., Hanganu, J., and David, L., "Synergy between lidar, radarsat-2, and spot-5 images for the detection and mapping of wetland vegetation in the danube delta," *IEEE Journal of Selected Topics in Applied Earth Observations and Remote Sensing* **9**(8), 3651–3666 (2016).

[41] Niculescu, S., Boissonnat, J.-B., Lardeux, C., Roberts, D., Hanganu, J., Billey, A., Constantinescu, A., and Doroftei, M., "Synergy of high-resolution radar and optical images satellite for identification and mapping of wetland macrophytes on the danube delta," *Remote Sensing* **12**(14), 2188 (2020).

[42] Rapinel, S., Panhelleux, L., Gayet, G., Vanacker, R., Lemercier, B., Laroche, B., Chambaud, F., Guelmami, A., and Hubert-Moy, L., "National wetland mapping using remote-sensing-derived environmental variables, archive field data, and artificial intelligence," *Heliyon* **9**(2) (2023).

[43] Huang, C., Peng, Y., Lang, M., Yeo, I.-Y., and McCarty, G., "Wetland inundation mapping and change monitoring using landsat and airborne lidar data," *Remote sensing of environment* **141**, 231–242 (2014).

[44] Mao, D., Wang, Z., Du, B., Li, L., Tian, Y., Jia, M., Zeng, Y., Song, K., Jiang, M., and Wang, Y., "National wetland mapping in china: A new product resulting from object-based and hierarchical classification of landsat 8 oli images," *ISPRS Journal of Photogrammetry and Remote Sensing* **164**, 11–25 (2020).

[45] Bhatnagar, S., Gill, L., Regan, S., Naughton, O., Johnston, P., Waldren, S., and Ghosh, B., "Mapping vegetation communities inside wetlands using sentinel-2 imagery in ireland," *International Journal of Applied Earth Observation and Geoinformation* **88**, 102083 (2020).

[46] Kaplan, G. and Avdan, U., "Mapping and monitoring wetlands using sentinel-2 satellite imagery," *ISPRS Annals of the photogrammetry, remote sensing and spatial information sciences* **4**, 271–277 (2017).

[47] Mahdianpari, M., Salehi, B., Mohammadimanesh, F., Homayouni, S., and Gill, E., "The first wetland inventory map of newfoundland at a spatial resolution of 10 m using sentinel-1 and sentinel-2 data on the google earth engine cloud computing platform," *Remote Sensing* **11**(1), 43 (2018).

[48] Jalbert, J., [*Coastal wetlands*], Océanopolis, Brest, France (2016).

[49] Kottek, M., Grieser, J., Beck, C., Rudolf, B., and Rubel, F., "World map of the köppen-geiger climate classification updated," (2006).

[50] Ministère de l'Écologie, du Développement Durable et de l'Énergie, Groupement d'Intérêt Scientifique Sol, "Guide for the identification and delimitation of wetland soils," rapport technique, Ministère de l'Écologie, du Développement Durable et de l'Énergie (2013).

[51] "Convention on wetlands of international importance especially as waterfowl habitat. ramsar (iran) (1971). united nations treaty series no. 14583." Retrieved from http://www.ramsar.org/cda/ramsar/display/main/main.jsp?zn=ramsar&cp=1-31-38^20671_4000_0__. (1971).

[52] Ellis, C. J., "Oceanic and temperate rainforest climates and their epiphyte indicators in britain," *Ecological Indicators* **70**, 125–133 (2016).

[53] DellaSala, D. A., DellaSala, D. A., Alaback, P., Spribille, T., von Wehrden, H., and Nauman, R. S., "Just what are temperate and boreal rainforests?," *Temperate and boreal rainforests of the world: Ecology and conservation* , 1–41 (2011).

[54] Galatowitsch, S. M., Whited, D. C., Lehtinen, R., Husveth, J., and Schik, K., "The vegetation of wet meadows in relation to their land-use," *Environmental monitoring and assessment* **60**, 121–144 (2000).

[55] Crowson, M., Warren-Thomas, E., Hill, J. K., Hariyadi, B., Agus, F., Saad, A., Hamer, K. C., Hodgson, J. A., Kartika, W. D., Lucey, J., et al., "A comparison of satellite remote sensing data fusion methods to map peat swamp forest loss in sumatra, indonesia," *Remote sensing in ecology and conservation* **5**(3), 247–258 (2019).

[56] Van Beijma, S., Comber, A., and Lamb, A., "Random forest classification of salt marsh vegetation habitats using quad-polarimetric airborne sar, elevation and optical rs data," *Remote Sensing of Environment* **149**, 118–129 (2014).

[57] Beninger, P. G., [*Mudflat ecology*], Springer (2018).

[58] Kelly, P. M. and White, J. M., "Preprocessing remotely sensed data for efficient analysis and classification," in [*Applications of Artificial Intelligence 1993: Knowledge-Based Systems in Aerospace and Industry*], **1963**, 24–30, SPIE (1993).

[59] Rouse Jr, J. W., Haas, R. H., Deering, D., Schell, J., and Harlan, J. C., "Monitoring the vernal advancement and retrogradation (green wave effect) of natural vegetation," tech. rep. (1974).

[60] Gitelson, A. A., Kaufman, Y. J., and Merzlyak, M. N., "Use of a green channel in remote sensing of global vegetation from eos-modis," *Remote sensing of Environment* **58**(3), 289–298 (1996).

[61] Gao, B.-C., "Ndwi—a normalized difference water index for remote sensing of vegetation liquid water from space," *Remote sensing of environment* **58**(3), 257–266 (1996).

[62] Rikimaru, A., Roy, P., and Miyatake, S., "Tropical forest cover density mapping," *Tropical ecology* **43**(1), 39–47 (2002).

[63] Baret, F., "Tsavi: a vegetation index which minimizes soil brightness effects on lai and apar estimation," in [*12th Canadian Symp. on Remote Sensing and IGARSS'90, Vancouver, Canada, 10-14 July 1989*], (1989).

[64] Sørensen, R., Zinko, U., and Seibert, J., "On the calculation of the topographic wetness index: evaluation of different methods based on field observations," *Hydrology and Earth System Sciences Discussions* **2**(4), 1807–1834 (2005).

[65] Merot, P., Hubert-Moy, L., Gascuel-Odoux, C., Clement, B., Durand, P., Baudry, J., and Thenail, C., "A method for improving the management of controversial wetland," *Environmental management* **37**, 258–270 (2006).

[66] Rapinel, S., Fabre, E., Dufour, S., Arvor, D., Mony, C., and Hubert-Moy, L., "Mapping potential, existing and efficient wetlands using free remote sensing data," *Journal of environmental management* **247**, 829–839 (2019).

[67] Cresson, R., "A framework for remote sensing images processing using deep learning techniques," *IEEE Geoscience and Remote Sensing Letters* **16**(1), 25–29 (2018).

[68] Adugna, T., Xu, W., and Fan, J., "Comparison of random forest and support vector machine classifiers for regional land cover mapping using coarse resolution fy-3c images," *Remote Sensing* **14**(3), 574 (2022).

[69] Zhu, T., "Analysis on the applicability of the random forest," in [*Journal of Physics: Conference Series*], **1607**(1), 012123, IOP Publishing (2020).

[70] Probst, P., Wright, M. N., and Boulesteix, A.-L., "Hyperparameters and tuning strategies for random forest," *Wiley Interdisciplinary Reviews: data mining and knowledge discovery* **9**(3), e1301 (2019).

[71] Breiman, L., "Bagging predictors," *Machine learning* **24**, 123–140 (1996).

[72] Blaschke, T., "Object based image analysis for remote sensing," *ISPRS journal of photogrammetry and remote sensing* **65**(1), 2–16 (2010).

[73] Hay, G. J. and Blaschke, T., "Geographic object-based image analysis (geobia)," *Photogramm. Eng. Remote Sens* **76**, 121 (2010).

[74] Wan, F. and Deng, F., "Remote sensing image segmentation using mean shift method," in [*International Conference on Computer Education, Simulation and Modeling*], 86–90, Springer (2011).

[75] Mehta, A. and Dikshit, O., "Segmentation-based projected clustering of hyperspectral images using mutual nearest neighbour," *IEEE Journal of Selected Topics in Applied Earth Observations and Remote Sensing* **10**(12), 5237–5244 (2017).

[76] Wu, Y.-c. and Feng, J.-w., "Development and application of artificial neural network," *Wireless Personal Communications* **102**, 1645–1656 (2018).

[77] Zhang, Z., Zhang, K., and Khelifi, A., [*Multivariate time series analysis in climate and environmental research*], Springer (2018).

[78] Zhu, X. X., Tuia, D., Mou, L., Xia, G.-S., Zhang, L., Xu, F., and Fraundorfer, F., "Deep learning in remote sensing: A comprehensive review and list of resources," *IEEE geoscience and remote sensing magazine* **5**(4), 8–36 (2017).

[79] Zhang, L., Zhang, L., and Du, B., "Deep learning for remote sensing data: A technical tutorial on the state of the art," *IEEE Geoscience and remote sensing magazine* **4**(2), 22–40 (2016).

[80] LeCun, Y., Bengio, Y., and Hinton, G., "Deep learning," *nature* **521**(7553), 436–444 (2015).

[81] Voulodimos, A., Doulamis, N., Doulamis, A., Protopapadakis, E., et al., "Deep learning for computer vision: A brief review," *Computational intelligence and neuroscience* **2018** (2018).

[82] Otter, D. W., Medina, J. R., and Kalita, J. K., "A survey of the usages of deep learning for natural language processing," *IEEE transactions on neural networks and learning systems* **32**(2), 604–624 (2020).

[83] Bae, H.-S., Lee, H.-J., and Lee, S.-G., "Voice recognition based on adaptive mfcc and deep learning," in [*2016 IEEE 11th Conference on Industrial Electronics and Applications (ICIEA)*], 1542–1546, IEEE (2016).

[84] Singh, S. P., Kumar, A., Darbari, H., Singh, L., Rastogi, A., and Jain, S., "Machine translation using deep learning: An overview," in [*2017 international conference on computer, communications and electronics (comptelix)*], 162–167, IEEE (2017).

[85] Zhao, Z.-Q., Zheng, P., Xu, S.-t., and Wu, X., "Object detection with deep learning: A review," *IEEE transactions on neural networks and learning systems* **30**(11), 3212–3232 (2019).

[86] Garcia-Garcia, A., Orts-Escolano, S., Oprea, S., Villena-Martinez, V., and Garcia-Rodriguez, J., "A review on deep learning techniques applied to semantic segmentation," *arXiv preprint arXiv:1704.06857* (2017).

[87] Minaee, S., Kalchbrenner, N., Cambria, E., Nikzad, N., Chenaghlu, M., and Gao, J., "Deep learning–based text classification: a comprehensive review," *ACM computing surveys (CSUR)* **54**(3), 1–40 (2021).

[88] Young, T., Hazarika, D., Poria, S., and Cambria, E., "Recent trends in deep learning based natural language processing," *ieee Computational intelligenCe magazine* **13**(3), 55–75 (2018).

[89] Hussain, J., "Deep learning black box problem," (2019).

[90] Panchal, G., Ganatra, A., Shah, P., and Panchal, D., "Determination of over-learning and over-fitting problem in back propagation neural network," *International Journal on Soft Computing* **2**(2), 40–51 (2011).

[91] Belgiu, M. and Drăguţ, L., "Random forest in remote sensing: A review of applications and future directions," *ISPRS journal of photogrammetry and remote sensing* **114**, 24–31 (2016).

[92] Storie, C. D. and Henry, C. J., "Deep learning neural networks for land use land cover mapping," in [*IGARSS 2018-2018 IEEE International Geoscience and Remote Sensing Symposium*], 3445–3448, IEEE (2018).

[93] Abdi, A. M., "Land cover and land use classification performance of machine learning algorithms in a boreal landscape using sentinel-2 data," *GIScience & Remote Sensing* **57**(1), 1–20 (2020).

[94] Günen, M. A., "Performance comparison of deep learning and machine learning methods in determining wetland water areas using eurosat dataset," *Environmental Science and Pollution Research* **29**(14), 21092–21106 (2022).

[95] Martineau, K., "Shrinking deep learning's carbon footprint," *MIT News* (2020).

[96] Ouyang, Z.-T., Zhang, M.-Q., Xie, X., Shen, Q., Guo, H.-Q., and Zhao, B., "A comparison of pixel-based and object-oriented approaches to vhr imagery for mapping saltmarsh plants," *Ecological informatics* **6**(2), 136–146 (2011).

[97] Mahdianpari, M., Granger, J. E., Mohammadimanesh, F., Warren, S., Puestow, T., Salehi, B., and Brisco, B., "Smart solutions for smart cities: Urban wetland mapping using very-high resolution satellite imagery and airborne lidar data in the city of st. john's, nl, canada," *Journal of environmental management* **280**, 111676 (2021).

[98] Boonpook, W., Tan, Y., Nardkulpat, A., Torsri, K., Torteeka, P., Kamsing, P., Sawangwit, U., Pena, J., and Jainaen, M., "Deep learning semantic segmentation for land use and land cover types using landsat 8 imagery," *ISPRS International Journal of Geo-Information* **12**(1), 14 (2023).

[99] Ronneberger, O., Fischer, P., and Brox, T., "U-net: Convolutional networks for biomedical image segmentation," in [*Medical Image Computing and Computer-Assisted Intervention–MICCAI 2015: 18th International Conference, Munich, Germany, October 5-9, 2015, Proceedings, Part III 18*], 234–241, Springer (2015).

[100] Simonyan, K. and Zisserman, A., "Very deep convolutional networks for large-scale image recognition," *arXiv preprint arXiv:1409.1556* (2014).

[101] Vapnik, V., [*The nature of statistical learning theory*], Springer science & business media (1999).

[102] Qi, J., Chehbouni, A., Huete, A. R., Kerr, Y. H., and Sorooshian, S., "A modified soil adjusted vegetation index," *Remote sensing of environment* **48**(2), 119–126 (1994).

[103] Matsushita, B., Yang, W., Chen, J., Onda, Y., and Qiu, G., "Sensitivity of the enhanced vegetation index (evi) and normalized difference vegetation index (ndvi) to topographic effects: a case study in high-density cypress forest," *Sensors* **7**(11), 2636–2651 (2007).

[104] Shahrayini, E. and Noroozi, A. A., "Modeling and mapping of soil salinity and alkalinity using remote sensing data and topographic factors: a case study in iran," *Environmental Modeling & Assessment* **27**(5), 901–913 (2022).